Peer-reviewed version available at *Nanomaterials* **2020**, *10*, 1717; doi:10.3390/nano10091717

Article

Gold Nanoparticles Radio-Sensitize and Reduce Cell Survival in Lewis Lung Carcinoma

Arvind Pandey [1], Veronica Vighetto [2,3], Nicola Di Marzio [2,4], Francesca Ferraro [2,3], Matteo Hirsch [2,3], Nicola Ferrante [2,5], Sankar Mitra [1], Alessandro Grattoni [1,2,6], and Carly S. Filgueira [2,7,*]

[1] Department of Radiation Oncology, Houston Methodist Research Institute, Houston, Texas, USA 77030;
[2] Department of Nanomedicine, Houston Methodist Research Institute, Houston, Texas, USA 77030;
[3] Department of Applied Science and Technology, Politecnico di Torino, Torino, IT 10129;
[4] Department of Electronic and Telecommunications, Politecnico di Torino, Torino, IT 10129;
[5] Department of Biomedical Engineering, Politecnico di Torino, Torino, IT 10129;
[6] Department of Surgery, Houston Methodist Research Institute, Houston, Texas, USA 77030;
[7] Department of Cardiovascular Surgery, Houston Methodist Research Institute, Houston, Texas, USA 77030;

* Correspondence: csfilgueira@houstonmethodist.org; Tel.: 713-441-1996 (C.S.F.)

Abstract: It has been suggested that particle size plays an important role in determining the genotoxicity of gold nanoparticles (GNPs). The purpose of this study was to compare the potential radio-sensitization effects of two different sized GNPs (3.9 and 37.4 nm) fabricated and examined in vitro in Lewis Lung carcinoma (LLC) as a model of non-small cell lung cancer through use of comet and clonogenic assays. After the treatment of 2Gy X-ray irradiation, both particle sizes demonstrated increased DNA damage when compared to treatment with particles only and radiation alone. This radio-sensitization was further translated into a reduction in cell survival demonstrated by clonogenicity. This work indicates that GNPs of both sizes induce DNA damage in LLC cells at the tested concentrations, whereas the 37.4 nm particle size treatment group demonstrated greater significance in vitro. The presented data aids in the evaluation of the radiobiological response of Lewis Lung carcinoma cells treated with gold nanoparticles.

Keywords: Gold Nanoparticles; Lewis Lung Carcinoma; Radio-Sensitization; Clonogenic Assay; Comet Assay

1. Introduction

Gold nanoparticles (GNPs) offer a means to transport agents to diseased cells or tissues because of their physical, chemical, and optical properties which are specifically dependent on size, adaptability, and biocompatibility[1]. They can also act as both cancer therapeutics and diagnostic tools, and have been demonstrated as novel molecular imaging contrast agents, computed tomography (CT) imaging, and photothermal cancer therapy[2,3]. The high atomic number of elemental gold (Z=79) compared to that of soft tissues, permits metal enhanced radiotherapy, where their presence can amplify delivered ionizing radiation. Current theory suggests that gold nanoparticle-mediated radio-sensitization is a combination of physical, chemical, and biological effects. On the physical side, multiple effects occur including the generation of photoelectrons, Auger electrons, and low energy secondary electrons. These emissions produce ionization effects in the neighboring tissues[4]. In addition, GNP-mediated radio-enhancement is likely due to modulation in cell cycle and increased production of reactive oxygen species (ROS), where enhanced localized absorption of X-rays results in energy deposition in the form of free radicals and electrons, causing cell damage[5]. However, it is still unclear how significantly a difference in particle size can affect the degree of radio-enhancement since size can affect cellular uptake. Leung *et al.*[6] use Monte Carlo simulation and show that GNPs with greater sizes increase the generation of the secondary electrons.

Experimentally, Brun *et al.*[7] conclude that with a constant effective X-ray energy of 49 keV, larger sized GNPs (92 nm) were more efficient radiosensitizers than those of smaller diameter (8 nm). However, Butterworth *et al.*[8] discuss that for smaller (5 and 20 nm) particles, the chemical yields of DNA damage in irradiated samples were significantly greater than that for 1.5 μm particles. Because of this discrepancy in the literature in size, in this work two different sized GNPs are assessed as radio-sensitizers in lung cancer cells.

Here, we exploit GNPs because of their desirable optical and electronic properties which make them an excellent absorber of X-rays. We sought to assess the *in vitro* radiobiological response of Lewis Lung carcinoma (LLC) treated with low dose (2Gy) x-ray irradiation alone and in combination with two different sized gold nanoparticles to evaluate GNP-mediated effects. The aim of this study was to determine if GNPs result in greater DNA damage in lung cancer cells in the presence of irradiation and if modifying particle size resulted in differences in the radiobiological response.

2. Materials and Methods

Synthesis of Gold Nanoparticles (GNPs)

Small GNPs (SGNP) were synthesized according to Duff *et al.*[9] using Tetrakis(hydroxymethyl)phosphonium chloride (Sigma-Aldrich, 404861) and Hydrogen tetrachloroaurate(III) hydrate (Sigma-Aldrich, 254169). Particles were also observed and measured on a Bruker Multimode Atomic Force Microscope (AFM) to yield a size of approximately 3.86 ± 1.27 nm. Z-potential values of -55.6 ± 13.5 mV were obtained, which confirm the layer of absorbed citrate anions. Citrate stabilizes the particles, minimizing aggregation. These anions can be displaced by wet chemistry to fabricate highly ordered arrays[10] self-assembled monolayers,[11] or hybrid lipid bilayers[12].

Big GNPs (BGNP) were synthesized using citric acid (Sigma, C3674) and Gold (III) Chloride (Sigma, 379948). Briefly, 600 ul of MilliQ was added to an Erlenmeyer flask and placed on a hot plate until vigorous boiling. After 30s of refluxing, 4.8 ml of 0.039 M aqueous citrate was added to the flask. Finally, after about one minute, 7 ml of 0.033 M Gold (III) Chloride was rapidly added to the boiling solution and left on the hot plate for four minutes until the observed color change was complete. The solution equilibrated to room temperature and was stored for further use. Dynamic Light Scattering (DLS) was used to rapidly and qualitatively size the particles and obtain a polydispersity index (PDI) and Zeta Potential was measured (Malvin). The solutions yield Z-potentials of -40.0 ± 6.0 mV (5 replicates in 10 mM KCl solution where the result is reported as mean ± SD). Particles were also observed and measured on a FEI Nova NanoSEM 230 and a JOEL 1230 High Contrast TEM, yielding an average particle diameter of 37.39 ± 5.52 nm.

Cell Culture

Murine Lewis Lung cells (LLC) were obtained from ATCC® (Manassas, VA, USA) and subcultured according to manufacturer's recommended protocols, where the complete growth medium consisted of DMEM with 10% FBS and subcultures were prepared by diluting the suspensions 1:4 to 1:6 using 0.25% trypsin - 0.53 mM EDTA solution (Thermo Fisher Scientific, Waltham, MA USA). Cells were made to express luciferase by the use of plasmid pLenti PGK V5-LUC Neo[13] (Addgene, Cambridge, MA, USA) which was packaged in lentiviral particles. The packaging was performed at the Baylor College of Medicine (BCM) vector core facility. The plasmid was transfected into Human Embryonic Kidney (HEK-293T) cells, and the conditioned media collected and used to infect the LLC1 for 24h. After 24h, selection was initiated with G418 (Geneticin, ThermoFisher Scientific, Waltham, MA, USA). Dulbecco's Modified Eagle's Medium (DMEM, ATCC®, Manassas, VA, USA) was made complete by adding 10% fetal bovine serum (FBS, USDA approved, ATCC®, Manassas, VA, USA) and 1% Geneticin™ (ThermoFisher Scientific, Waltham, MA, USA) for the luciferase expressing cells to maintain culture. Cells were kept at 37 ºC and 5% humidity in HERAcell 150i CO2 incubator (ThermoFisher Scientific, Waltham, MA, USA).

Comet Assay

A neutral comet assay was performed using a CometAssay® Kit (Trevigen, Gaithersburg, MD, USA) as per manufacturer's instruction to detect DNA damage due to irradiation. Briefly LLC were incubated with 54.5 μg of either SGNP or BGNP for 48 hrs and irradiated with 2Gy using a Rad Source RS-2000 Biological Research Irradiator (Buford, GA, USA). Thirty minutes after irradiation cells were collected, counted, and mixed with 0.5% low melting point (LMP) agarose and spread over the comet slide. Slides were then immersed in an ice-cold freshly prepared lysis solution for at least 1 h. The slides were taken out of the lysis solution and then placed in a cold 1x neutral electrophoresis buffer for 30 minutes. Horizontal electrophoresis was performed at 4°C in low light conditions for 45 min at 21 V. Following the electrophoresis protocol, the slides were next immersed in DNA Precipitation Solution for 30 minutes and 70% ethanol for 30 min at room temperature. Each slide was dried with air and stained with 1x SYBR® Gold Staining Solution (Trevigen, Gaithersburg, MD, USA) in the dark. All slides were washed with water and air dried. Samples were visualized using an EVOS FL Auto microscope (Life Technology). DNA damage was quantified by evaluating both tail length (defined as the length of DNA migration and is related to DNA fragment size, calculated from the center of the cell and reported in micrometers) and tail moment (determined by tail length times the fraction of DNA in the tail). At least 50 random cells were scored per sample. Image was analyzed by Open Comet plugin in ImageJ for various comet parameters[14].

Clonogenic Assay

LLC cells were treated with 54.5 μg of either SGNP or BGNP for 48 hrs followed by 2Gy radiation alone and combined with NP treatment using a Rad Source RS-2000 Biological Research Irradiator (Buford, GA, USA). Thirty minutes after irradiation cells were trypsinized and approximately 200-500 cells from each sample were plated in triplicate in 6-well plates. After 10-15 days, the colonies were stained with 0.5% crystal violet solution in 50% methanol. Clonogenic efficiency was measured by % area and/or % intensity through colony area plugin (ImageJ)[15].

Statistical Analysis

GraphPad Prism 5 software was used for all statistical analyses. Data are expressed as the median with interquartile range for comet assay and mean ± SD in clonogenic assay. Asterisks denote P-values in the figures and sample sizes are included in each figure legend. One-way ANOVA was used to determine statistical significance.

3. Results and discussion

3.1. Characterization and physicochemical properties of the SGNPs and BGNPs

Two different sized gold nanoparticles small (SGNP) and big (BGNP) were synthesized (Fig. 1) and investigated for radio-sensitization effects *in vitro*. While particles of both sizes displayed similar optical absorption spectra (Fig. 1A), they appeared different in color to the visible eye (Fig. 1C, 1D) and measured a ten-fold difference in diameter (Fig. 1B, 1E-H). At this size range, the NPs can be internalized by LLC cells via endocytosis into cells (Fig. 1I, 1J). The particle clusters remain within vacuoles within the cell (highlighted by red arrows). Even without a targeting moiety, macropinocytosis of the SGNP can be clearly seen in the top right of Fig. 1I. This is one of four types of endocytosis pathways and is a non-specific process to internalized fluids and particles together into the cells[16]. This observed efficiency in penetrating cells is one of the unique properties of GNPs[17] which we choose to exploit here for radiotherapy.

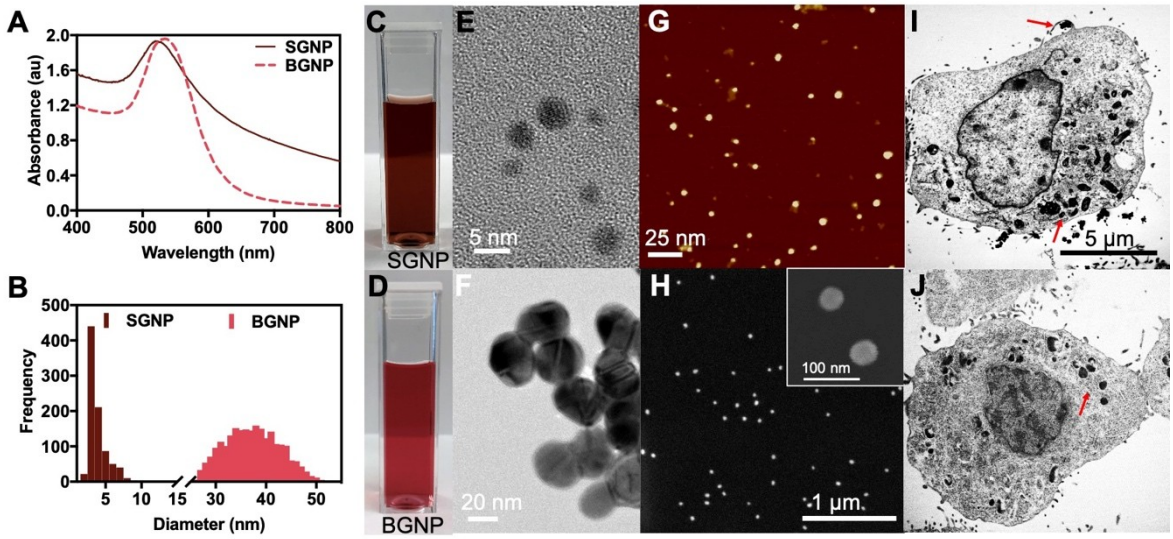

Figure 1. (**A**) Absorbance spectra of the small (SGNP) and big (BGNP) gold nanoparticles with an absorbance maxima occurring around 534 and 519 nm, respectively. (**B**) Size distributions of SGNP (average particle size of 3.86 ± 1.27 nm) and BGNP (average particle size 37.39 ± 5.52 nm) for over 300 particles. Optical photo of (**C**) SGNP and (**D**) BGNP. TEM images of (**E**) SGNP and (**F**) BGNP. (**G**) AFM image of the SGNP and (**H**) SEM image of the BGNP. (**I**) SGNP and (**J**) BGNP internalized in LLC cells.

3.2. Effects of gold nanoparticles (SGNP and BGNP) with radiation on DNA damage in LLC cells

The comet assay offers a robust technique to evaluate DNA damage in cells and has been broadly used to measure both DNA damage and repair *in vitro* after genotoxic stress.[18] Once an electric field is applied, denatured and cleaved DNA fragments migrate out of the nucleoid with more damaged DNA migrating faster yielding a "comet" tail shape. For a neutral comet assay, damage is assessed through double-stranded breaks in DNA. Figure 2A shows the visualization of a neutral comet assay by epifluorescence microscopy performed on untreated (UT) LLC cells and cells treated with SGNPs and BGNPs only, irradiated (XRT-2Gy) cells, and combined treatment of radiation with SGNPs or BGNPs. It should be noted that the amount of gold incubated with the cells for both the SGNP and BGNP treatment groups was kept constant (54.5 µg/well in a 6-well plate with a surface area of 9 cm^2 per well). Undamaged DNA remains in the head of the "comet", and the tail represents the amount of damaged DNA (or charged DNA) that migrates in an electric field. A dose of 2Gy was chosen as it is not only a typical dose used in the literature[19–21] but also showed significance in modifying the tail moment when compared to the untreated cells with evidence of a synergistic effect when GNPs were present.

When plotted as a function of tail moment, no significant difference was observed between the UT and SGNP groups however a significant (*$p<0.033$) increase in DNA damage was found in the BGNP group when compared to UT cells. Researchers have noticed size dependent toxicity of gold nanoparticles,15 but it is dependent on assay type, cell line, and nanoparticle properties, leading to conflicting results. As evident, a significant difference in DNA damage was observed (**$p<0.002$) between the UT and radiation only (XRT-2Gy) treated group. Further, synergistic increase of DNA damage (***$p<0.001$) was observed in combinatorial treatment of radiation with either of SGNPs and BGNPs (SGNP XRT-2Gy or BGNP XRT-2Gy). When both particles are compared to each other, the significant difference was seen in both irradiated and non-irradiated groups. It is not surprising that exposure to radiation resulted in evidence of a higher tail moment compared to the untreated group, since ionizing radiation is known to produce double-stranded breaks due to the physico-chemical interaction with cellular DNA.[18] However, overall, the greater tail moment for the cells irradiated

in the presence of gold nanoparticles indicates that for these two treatment groups, DNA damage was more significant with respect to radiation alone.

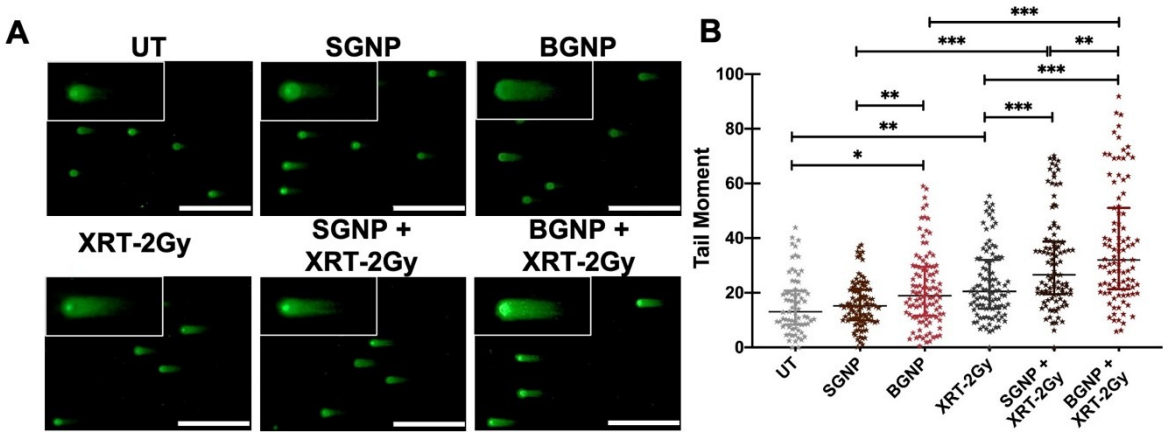

Figure 2. Neutral comet assay for LLC cells. Cells were untreated (UT), treated with small gold nanoparticles (SGNP) or big gold nanoparticles (BGNP), 2Gy x-ray irradiation (XRT-2Gy), or a combination of 2Gy and either small or big gold nanoparticles. (**A**) Scale bar represents 400 μm. (**B**) The horizontal line shows the median and the vertical line shows the interquartile range. At least 50 random cells were scored per sample. A one-way ANOVA was performed to determine statistical significance (*p<0.033, **p<0.002, and ***p<0.001).

3.2. Effects of gold nanoparticles (SGNP and BGNP) with radiation on LLC cell survival

The clonogenic assessment (Fig. 3) showed that the ability of cells to replicate decreased significantly after treatment with BGNPs and radiation. In contrast, combinatorial treatment of radiation with both particles further significantly reduced the cell survival. However, we did not observe any significant difference between SGNPs and BGNPs. While the presence of GNPs did not visibly alter the proliferation of the cells into colonies, a reduction in the number of cells can be seen when treated with irradiation alone and combination of GNPs and irradiation (Fig. 3A).

When the data is represented as a function of the normalized percent area (Fig. 3B), statistical significance can be evaluated for the different groups. The three control groups, UT, SGNP, and BGNPs, all show a normalized percent area within error of each other. In the presence of irradiation, however, significance (***p<0.001) is observed between the UT and XRT-2Gy groups as well as significance (***p<0.001) between the SGNP and XRT-2Gy and BGNP and XRT-2Gy groups is observed. In combinatorial treatment of radiation with either of SGNPs and BGNPs (SGNP XRT-2Gy or BGNP XRT-2Gy) a significance of (***p<0.001) is found when compared with the XRT-2Gy radiation alone again demonstrating a synergistic effect when combined. When combined with irradiation, the presence of the particles decreased the % area by 36% and 39% for the SGNP and BGNP, respectively as compared to the radiation alone (XRT-2Gy) group.

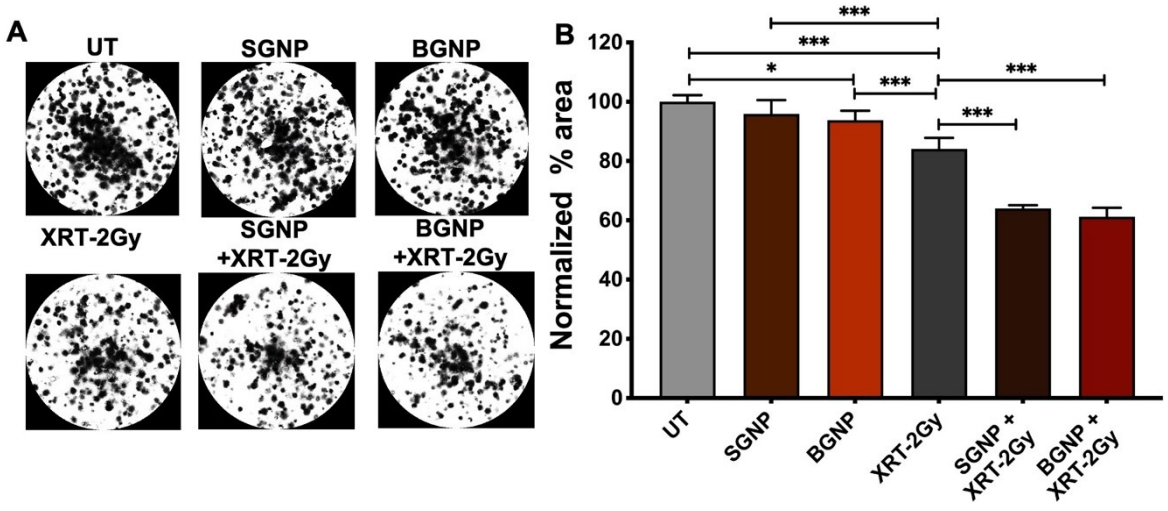

Figure 3. (**A**) Clonogenic assay performed *in vitro* with LLC to measure the survival potential after the various treatment paradigms. (**B**) Normalized % area for the different treatment groups. Cells from each sample were plated in triplicate. A one-way ANOVA was performed to determine statistical significance (*p<0.033, **p<0.002, and ***p<0.001).

4. Conclusions

In summary, GNPs of two different dimensions were fabricated to examine if GNPs could act as effective radio-sensitizers in vitro in a non-small cell lung cancer model. Comet and clonogenic assays performed with Lewis Lung carcinoma cells demonstrated that both sizes of the GNPs showed significant radio-sensitization and reduce cell survival after treatment. Greater significance was observed in vitro with the BGNP treatment group. Further in vivo evaluation of the effects of GNPs on radiation enhancement may help with the translation of these particles toward use in a clinical setting.

Author Contributions: Conceptualization, C.S.F., A.G. and A.P.; methodology, C.S.F. and A.P.; formal analysis, C.S.F. and A.P.; investigation, C.S.F.; resources, C.S.F., A.G. and S.M.; data curation, A.P., V.V., N.D.M, F.F., M.H., N.F. and C.S.F.; writing—original draft preparation, A.P. and C.S.F.; writing—review and editing, A.P., A.G. and C.S.F.; supervision, A.G. and C.S.F.; funding acquisition, C.S.F., A.G. and S.M. All authors have read and agreed to the published version of the manuscript.

Funding: This research was funded by the Simmons foundation (A.G.), Golfers Against Cancer (A.G. and C.S.F.), and funds from Houston Methodist Research Institute (S.M., A.G. and C.S.F.).

Acknowledgments: The authors would like to thank James Gu, Wei Jiang, and Weihua Gao for help with AFM, SEM, and TEM imaging, and Corrine Ying Xuan Chua, E. Brian Butler, Danilo Demarchi, and Naomi Halas (NH).

Conflicts of Interest: The authors declare no conflict of interest. The funders had no role in the design of the study; in the collection, analyses, or interpretation of data; in the writing of the manuscript, or in the decision to publish the results.

References

1. Arvizo, R.; Bhattacharya, R.; Mukherjee, P. Gold nanoparticles: opportunities and challenges in nanomedicine. *Expert Opinion on Drug Delivery* **2010**, *7*, 753–763, doi:10.1517/17425241003777010.
2. Huang, X.; El-Sayed, I.H.; Qian, W.; El-Sayed, M.A. Cancer Cell Imaging and Photothermal Therapy in the Near-Infrared Region by Using Gold Nanorods. *J. Am. Chem. Soc.* **2006**, *128*, 2115–2120, doi:10.1021/ja057254a.

3. Popovtzer, R.; Agrawal, A.; Kotov, N.A.; Popovtzer, A.; Balter, J.; Carey, T.E.; Kopelman, R. Targeted gold nanoparticles enable molecular CT imaging of cancer. *Nano Lett.* **2008**, *8*, 4593–4596.
4. Her, S.; Jaffray, D.A.; Allen, C. Gold nanoparticles for applications in cancer radiotherapy: Mechanisms and recent advancements. *Advanced Drug Delivery Reviews* **2017**, *109*, 84–101, doi:10.1016/j.addr.2015.12.012.
5. Babaei, M.; Ganjalikhani, M. The potential effectiveness of nanoparticles as radio sensitizers for radiotherapy. *Bioimpacts* **2014**, *4*, 15–20, doi:10.5681/bi.2014.003.
6. Leung, M.K.K.; Chow, J.C.L.; Chithrani, B.D.; Lee, M.J.G.; Oms, B.; Jaffray, D.A. Irradiation of gold nanoparticles by x-rays: Monte Carlo simulation of dose enhancements and the spatial properties of the secondary electrons production: Monte Carlo simulation on gold nanoparticles. *Medical Physics* **2011**, *38*, 624–631, doi:10.1118/1.3539623.
7. Brun, E.; Sanche, L.; Sicard-Roselli, C. Parameters governing gold nanoparticle X-ray radiosensitization of DNA in solution. *Colloids and Surfaces B: Biointerfaces* **2009**, *72*, 128–134, doi:10.1016/j.colsurfb.2009.03.025.
8. Butterworth, K.T.; Wyer, J.A.; Brennan-Fournet, M.; Latimer, C.J.; Shah, M.B.; Currell, F.J.; Hirst, D.G. Variation of Strand Break Yield for Plasmid DNA Irradiated with High- *Z* Metal Nanoparticles. *Radiation Research* **2008**, *170*, 381–387, doi:10.1667/RR1320.1.
9. Duff, D.G.; Baiker, A.; Edwards, P.P. A new hydrosol of gold clusters. 1. Formation and particle size variation. *Langmuir* **1993**, *9*, 2301–2309, doi:10.1021/la00033a010.
10. Wang, H.; Levin, C.S.; Halas, N.J. Nanosphere Arrays with Controlled Sub-10-nm Gaps as Surface-Enhanced Raman Spectroscopy Substrates. *J. Am. Chem. Soc.* **2005**, *127*, 14992–14993, doi:10.1021/ja055633y.
11. Levin, C.S.; Janesko, B.G.; Bardhan, R.; Scuseria, G.E.; Hartgerink, J.D.; Halas, N.J. Chain-Length-Dependent Vibrational Resonances in Alkanethiol Self-Assembled Monolayers Observed on Plasmonic Nanoparticle Substrates. *Nano Lett.* **2006**, *6*, 2617–2621, doi:10.1021/nl062283k.
12. Levin, C.S.; Kundu, J.; Janesko, B.G.; Scuseria, G.E.; Raphael, R.M.; Halas, N.J. Interactions of Ibuprofen with Hybrid Lipid Bilayers Probed by Complementary Surface-Enhanced Vibrational Spectroscopies. *J. Phys. Chem. B* **2008**, *112*, 14168–14175, doi:10.1021/jp804374e.
13. Campeau, E.; Ruhl, V.E.; Rodier, F.; Smith, C.L.; Rahmberg, B.L.; Fuss, J.O.; Campisi, J.; Yaswen, P.; Cooper, P.K.; Kaufman, P.D. A Versatile Viral System for Expression and Depletion of Proteins in Mammalian Cells. *PLoS ONE* **2009**, *4*, e6529, doi:10.1371/journal.pone.0006529.
14. Gyori, B.M.; Venkatachalam, G.; Thiagarajan, P.S.; Hsu, D.; Clement, M.-V. OpenComet: An automated tool for comet assay image analysis. *Redox Biology* **2014**, *2*, 457–465, doi:10.1016/j.redox.2013.12.020.
15. Guzmán, C.; Bagga, M.; Kaur, A.; Westermarck, J.; Abankwa, D. ColonyArea: An ImageJ Plugin to Automatically Quantify Colony Formation in Clonogenic Assays. *PLoS ONE* **2014**, *9*, e92444, doi:10.1371/journal.pone.0092444.
16. Park, J.H.; Oh, N. Endocytosis and exocytosis of nanoparticles in mammalian cells. *International Journal of Nanomedicine* **2014**, 51, doi:10.2147/IJN.S26592.
17. Xie, X.; Liao, J.; Shao, X.; Li, Q.; Lin, Y. The Effect of shape on Cellular Uptake of Gold Nanoparticles in the forms of Stars, Rods, and Triangles. *Scientific Reports* **2017**, *7*, doi:10.1038/s41598-017-04229-z.

18. Garaj-Vrhovac, V.; Kopjar, N. The alkaline Comet assay as biomarker in assessment of DNA damage in medical personnel occupationally exposed to ionizing radiation. *Mutagenesis* **2003**, *18*, 265–71.
19. Dunne, A.L.; Price, M.E.; Mothersill, C.; McKeown, S.R.; Robson, T.; Hirst, D.G. Relationship between clonogenic radiosensitivity, radiation-induced apoptosis and DNA damage/repair in human colon cancer cells. *British Journal Of Cancer* **2003**, *89*, 2277.
20. Palyvoda, O.; Polanska, J.; Wygoda, A.; Rzeszowska-Wolny, J. DNA damage and repair in lymphocytes of normal individuals and cancer patients: studies by the comet assay and micronucleus tests. *Acta Biochim Pol* **2003**, *50*, 181–90, doi:035001181.
21. Kurashige, T.; Shimamura, M.; Nagayama, Y. Differences in quantification of DNA double-strand breaks assessed by 53BP1/γH2AX focus formation assays and the comet assay in mammalian cells treated with irradiation and N-acetyl-L-cysteine. *Journal of Radiation Research* **2016**, *57*, 312–317, doi:10.1093/jrr/rrw001.